DOI: 10.1002/vms3.598

CASE REPORT

WILEY

Computed tomography may detect liver infiltration of canine diffuse hepatic lymphoma

Toshiyuki Tanaka[1,2] | Hiroki Yamazaki[1] | Kazuna Ashida[1] | Yasumasa Iimori[1] | Keiichiro Mie[1] | Hidetaka Nishida[1] | Hideo Akiyoshi[1]

[1] Laboratory of Veterinary Surgery, Graduate School of Life and Environmental Sciences, Osaka Prefecture University, Izumisano-shi, Osaka, Japan

[2] Kinki Animal Medical Training Institute & Veterinary Clinic, Higashiosaka, Osaka, Japan

Correspondence
Dr Hideo Akiyoshi, Laboratory of Veterinary Surgery, Division of Veterinary Science, Graduate School of Life and Environmental Sciences, Osaka Prefecture University, 1–58 Rinku, Ohrai-kita, Izumisano, Osaka 598–8531, Japan.
Email: akiyoshi@vet.osakafu-u.ac.jp

Abstract

Background: In dogs, hepatic lymphoma is characterized by neoplastic lymphocyte infiltration into the liver. Reports on the computed tomography (CT) findings of the liver for canine hepatic lymphoma are few, with only one study of multiple liver lesions type.

Objectives: The purpose of this study was to retrospectively assess the CT findings of the liver in canine diffuse hepatic lymphoma.

Methods: As control, five dogs without abnormalities in the liver were included. CT data were analysed, and the following were noted: presence of edge bluntness of the liver, presence of periportal collar sign, the liver size:body weight (BW) ratio and the mean attenuation of liver lesions on pre-contrast, arterial-phase, portal-phase and equilibrium-phase post-contrast images.

Results: On CT examination, edge bluntness of the liver was significantly detected in lymphoma (4/5, 80%), as opposed to the control (0/5, 0%) ($p = 0.048$, $\varphi = 0.82$). The periportal collar sign was detected in lymphoma (3/5, 60%), as opposed to the control (0/5, 0%) ($p = 0.17$, $\varphi = 0.65$). The liver size:BW ratio of lymphoma cases was significantly higher compared to that of the control cases ($p = 0.0002$, $r = 0.92$). The mean Hounsfield unit of lymphoma cases in the pre-contrast, arterial-phase, portal-phase and equilibrium-phase images were significantly lower than in the control cases ($p = 0.005$, $r = 0.81$; $p = 0.0003$, $r = 0.91$; $p = 0.01$, $r = 0.75$ and $p = 0.02$, $r = 0.71$, respectively).

Conclusions: Hepatic lymphoma should be a differential for a blunted and enlarged liver with hypoattenuation on CT examination.

KEYWORDS
diagnosis, dog, hepatic disease, imaging-CT

1 | INTRODUCTION

In dogs, hepatic lymphoma is characterized by the infiltration of neoplastic lymphocytes into the liver by several form of lymphoma such as multicentric, alimentary, cranial mediastinal and extranodal forms (Cullen, 2017; Nyland, 1984). To diagnose lymphoma, ultrasonography and cytology are available as routine techniques (Nerschbach et al., 2016). Ultrasonographic findings of hepatic lymphoma include hypo to isoechoic lesions, diffuse hypo to normal echogenicity and diffuse hyperechogenicity compared to normal liver or reference organ such as spleen and right kidney with hepatomegaly (Lamb et al., 1991; Nyland, 1984; Whiteley et al., 1989; Wrigley et al., 1988). These findings are similar to those of other tumours, including histiocytic neoplasms, mast cell disease or hemangiosarcoma (Cruz-Arambulo et al., 2004; O'brien, 2007; Ramirez et al., 2002; Sato & Solano, 2004). Cytology of liver lesions, especially lymphoma, is a valuable diagnostic tool (Roth, 2001). The limitation of cytology involves the risk of inadequate or unrepresentative sampling (Nerschbach et al., 2016). In dogs, the positive predictive value and sensitivity for detecting neoplasia of liver by cytology is 86.7% and 52.0%, respectively (Bahr et al., 2003). In humans, computed tomography (CT) is performed to diagnose hepatic lymphoma, which is classified as solitary lesion, multiple lesions and diffuse lesions (Maher et al., 2001). In hepatic lymphoma, lesions are hypoattenuating on pre-contrast and have either no contrast enhancement (50%), patchy enhancement (33%) and ring enhancement (16%) (Ippolito et al., 2020, Maher et al., 2001). In dogs, information is limited on the CT findings of the liver for canine hepatic lymphoma. The purpose of this study was to retrospectively assess the CT findings of the liver in canine diffuse hepatic lymphoma.

2 | MATERIALS AND METHODS

This study had a retrospective case series. In this study, five dogs with hepatic lymphoma that underwent CT examination were used. As a control, five dogs with disc herniation or urinary bladder stones were used. Although liver biopsy was not performed, these five dogs were clinically diagnosed no liver abnormalities by biochemistry profile and follow up CT. All dogs underwent general anaesthesia with a ventilator and were placed in the supine position during CT examinations. A stop ventilator-induced apnoea during the acquisitions and total body scans were performed for all dogs. CT was performed using a multidetector 16-slice CT scanner (SOMATOM Scope; SIEMENS, Tokyo, Japan) in the helical scan mode according to our usual protocol. The CT was performed with a pitch of 0.65, scan thickness of 1.2 mm, 100–150 mAs, 120 kV, patient size-adjusted display FOV and soft tissue reconstruction filters. Images were reconstructed at 2-mm slice thickness using soft tissue filters and pulmonary filters. For contrast-enhanced imaging, all dogs were administered with 2 ml/kg of nonionic contrast medium (300 mg/ml Ioverin 300; Teva Pharma Japan, Inc., Aichi, Japan) via an indwelling intravenous cannula placed in the cephalic vein. The injection time was 20 s. Post-contrast studies were performed during the arterial (20 s after the start of contrast injection), portal (60 s after the start of contrast injection) and equilibrium (180 s after the start of contrast injection) phases. For image analyses, CT images were displayed with a window level of 35 Hounsfield unit (HU) and a window width of 360 HU on a computer workstation using commercially available DICOM image viewing software (Horos software ver. 2.4.1, Horos Project, Annapolis, MD, USA). All CT images were reviewed by two experienced veterinary radiologists, and the CT features were recorded by consensus. Observers were not aware of the final diagnoses at the time of the CT image review. All studies were assessed in a random order to minimize potential bias.

The following CT parameters were recorded: presence number, location, presence of edge bluntness of the liver, presence of periportal collar sign and the liver size:body weight (BW) ratio. By referring to the edge bluntness that defined by ultrasonography, the edge bluntness on CT was defined in any reformatted plane (Nishiura et al., 2005). The periportal collar sign was defined as areas of low attenuation around the portal vein and its branches (Takeda et al., 2015). The liver size:BW ratio was measured using similar techniques that are reported in the literature (Lee et al., 2019). Liver area was calculated using a manually drawing regions of interest (ROI) on each transverse CT image, excluding the gallbladder. Total liver volume was calculated from these ROIs using DICOM image viewing software (Horos software ver. 2.4.1). The liver size:BW ratio was determined by total liver volume /BW(kg). The mean attenuation of liver lesions of lymphoma as well as attenuation of the control liver parenchyma was measured on pre-contrast, arterial-phase, portal-phase and equilibrium-phase post-contrast images by manually drawing the ROI 3 times to fit the liver lesion. The mean HU of the liver and standard deviation (SD) values in the pre-contrast, arterial-phase, portal-phase and equilibrium-phase images were calculated. The mean HU of aorta and SD values in each phase images were calculated as an internal control at the cross-section of the liver lesion.

Statistical calculations were performed using R version 2.12.1 (R Development Core Team, 2010. R: a language and environment for statistical computing. R Foundation for Statistical Computing, Vienna, Austria. ISBN 3-900051-07-0. Available at: http://www.R-project.org/. Accessed on February 11, 2011). Normalization of quantitative CT data was assessed using the Shapiro–Wilk test, which indicated that parametric testing was required. Results with p-values less than 0.05 were considered significant. The difference in qualitative parameters between the lymphoma and control group was assessed using Fisher's exact test. On the liver size:BW ratio and the attenuation of pre-contrast and each post-contrast image, the differences between lymphoma and control were assessed using a 2-tailed unpaired t-test. To assist in determining between-group differences, effect size statistics on Fisher's exact test (φ) and 2-tailed unpaired t-test (r) were calculated for each dependent variable. An effect size of 0.5 or larger was defined as meaningful difference (Cohen, 1988a; Cohen, 1988b).

3 | RESULT

The lymphoma group comprised five intact male dogs. The mean (±SD) age of the dogs with lymphoma was 8.4 ± 2.5 years. The dog breeds included Bernese Mountain Dog, Shih Tzu, Maltese, Yorkshire

TABLE 1 Clinical findings of five dogs with lymphoma

Breed	Sex	Age (year)	Clinical signs	GPT, ALKP	T-Bil
Bernese Mountain Dog	MI*	5	Weight loss	261, 86	0.2
Shih Tzu	MI	12	Lethargy Anorexia	>1000, > 3500	1.4
Maltese	MI	8	Lethargy Anorexia	597, > 3500	12.3
Yorkshire Terrier	MI	9	Lethargy Anorexia	111, 251	0.1
German Shepherd	MI	8	Lethargy Anorexia	577, 2065	0.3

*MI: male intact, GPT (reference interval: 17–78 U/L), ALKP (reference interval: 47–254 U/L), T-Bil (reference interval: 0.1–0.5 mg/dl).

TABLE 2 CT features of liver

CT features	Lymphoma $N = 5$	Control $N = 5$	p Value	Effect size φ
Edge bluntness				
Present	4/5 (80%)	0/5 (0%)	0.048*	0.82
Absent	1/5 (20%)	5/5 (100%)		
Periportal collar sign				
Present	3/5 (60%)	0/5 (0%)	0.17	0.65
Absent	2/5 (40%)	5/5 (100%)		

*$p < 0.05$.
CT, computed tomography.

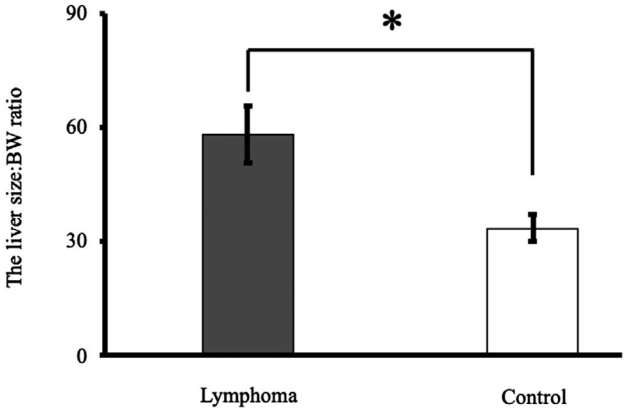

FIGURE 1 The liver size:BW ratio of lymphoma and control cases (*$p < 0.05$)

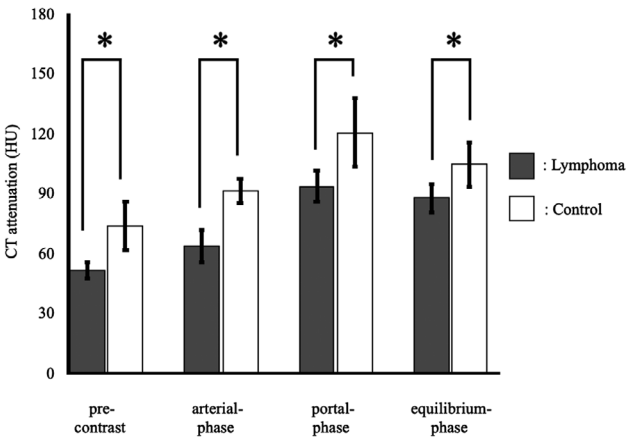

FIGURE 2 Computed tomographic attenuation values of liver in hepatic lymphoma and control cases on pre-contrast, arterial, portal and equilibrium phase post-contrast images (*$p < 0.05$)

Terrier and German Shepherd. One dog presented with weight loss and four dogs presented with lethargy and anorexia. On physical exam, peripheral lymphadenopathy was not detected in all dogs. All dogs had increased Glutamic Pyruvic Transaminase (GPT) (range: 111–over measure limit U/L; reference interval: 17–78 U/L). Three dogs had increased Alkaline Phosphatase (ALKP) (range: 2065–over measure limit U/L; reference interval: 47–254 U/L). Two dogs had increased Total Bilirubin (T-Bil) (1.4 and 12.3 mg/dl; reference interval: 0.1–0.5 mg/dl). Clinical findings of five dogs with lymphoma were summarized in Table 1. Cytologic evaluation, as per a board-certified clinical pathologist, was consistent with lymphoma. The control group comprised three intact males, a spayed female and an intact female dog. The mean (±SD) age of control dogs was 6.2 ± 3.0 years. The dog breeds included three Miniature Dachshunds, a French bulldog and a medium mix breed.

On CT examination, all dogs with hepatic lymphoma showed diffuse hepatic lesions and no architectural distortion. Although biopsy was not performed, there were no abnormalities of other organ on CT examination. Edge bluntness of the liver was detected on all three planes in four (80%) and no (0%) dogs in the lymphoma and control groups respectively. The edge bluntness showed a significant difference between the lymphoma and control cases ($p = 0.048$, $\varphi = 0.82$). The periportal collar sign was detected in three (60%) and no (0%) dogs in the lymphoma and control groups, respectively. There was no significant difference in periportal collar sign between lymphoma and control cases although the periportal collar sign was more frequently detected in lymphoma compared to control cases ($p = 0.17$, $\varphi = 0.65$) (Table 2).

The liver size:BW ratio was 58.3 ± 7.5 and 33.6 ± 3.7 for lymphoma and control, respectively. The liver size:BW ratio of lymphoma cases was significantly higher compared to that of the control cases ($p = 0.0002$, $r = 0.92$) (Figure 1).

In the pre-contrast images, the mean HU was 51.7 ± 4.1 and 73.7 ± 12.1 for lymphoma and control, respectively. In the arterial-phase images, the mean HU was 63.7 ± 8.2 and 91.5 ± 6.0 for lymphoma and control, respectively. In the portal-phase images, the mean HU was 93.6 ± 7.7 and 120.4 ± 17.1 for lymphoma and control, respectively. In the equilibrium-phase images, the mean HU was 87.7 ± 7.2 and 104.6 ± 11.2 for lymphoma and control, respectively. The mean HU of

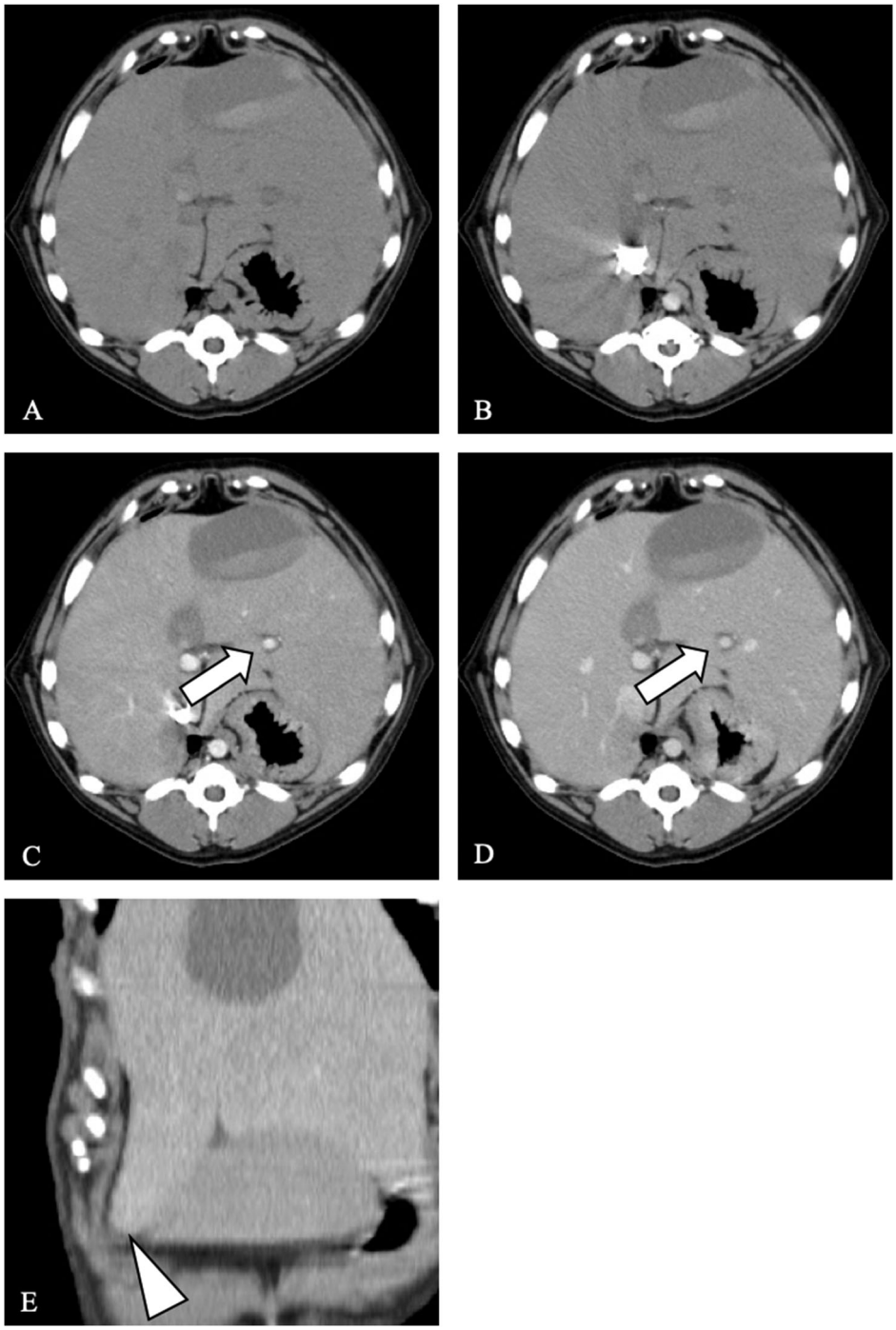

FIGURE 3 Representative axial pre-contrast (a), arterial (b), portal (c) and equilibrium (d) phase post-contrast CT images of diffuse hepatic lymphoma. All dogs with diffuse hepatic lymphoma showed no architectural distortion. The periportal collar sign (arrow) was detected in 60% of lymphoma cases. The edge bluntness of the liver (e, arrowhead) was detected in 80% of lymphoma cases

lymphoma cases in the pre-contrast, arterial-phase, portal-phase and equilibrium-phase images were significantly lower compared to that of the control cases ($p = 0.005$, $r = 0.81$; $p = 0.0003$, $r = 0.91$; $p = 0.01$, $r = 0.75$; and $p = 0.02$, $r = 0.71$, respectively) (Figure 2). In lymphoma cases, the mean HU of aorta in in the pre-contrast, arterial-phase, portal-phase and equilibrium-phase images were 39.4 ± 3.0, 348.8 ± 92.8, 149.6 ± 9.9 and 115.6 ± 12.5, respectively. In control cases, the mean HU of aorta in in the pre-contrast, arterial-phase, portal-phase and equilibrium-phase images were 43.4 ± 7.5, 385.6 ± 141.2, 166.2 ± 25.0 and 129.2 ± 14.3, respectively. The mean HU of aorta in each phase images showed no significant difference between lymphoma and control ($p = 0.3$, $r = 0.36$; $p = 0.64$, $r = 0.17$; $p = 0.21$, $r = 0.44$; and $p = 015$, $r = 0.49$, respectively). Representative images of the liver in canine hepatic lymphoma are shown in Figure 3.

4 | DISCUSSION

Hepatic lymphoma in humans can present as a solitary lesion, multifocally, or diffusely throughout the parenchyma (Maher et al., 2001). Solitary lesion is the most common, seen in approximately 60% cases of hepatic lymphoma, followed by multiple liver lesions in approximately 35%–40% (Rajesh et al., 2015; Tomasian et al., 2015). Diffuse lesions are rare and portend poor prognosis in human hepatic lymphoma (Rajesh et al., 2015). In this study, all liver lesions of canine hepatic lymphoma were diffuse lesions. To our knowledge, approximately 33%–55% cases of hepatic lymphoma are diffuse liver lesions in the dog (Nyland, 1984; Whiteley et al., 1989). One dog with diffuse hepatic lymphoma developed multiple nodules after therapy, 4 weeks after initial diagnosis (Chung et al., 2014). Canine hepatic lymphoma is extremely aggressive and has a poor response to therapy (Vail et al., 2013). Therefore, distinguishing diffuse hepatic lymphoma from other presentations of lymphoma, may be prognostically useful.

In this study, edge bluntness of the liver was detected in 80% of dogs with hepatic lymphoma. Edge bluntness of the liver is one of the ancillary signs of hepatomegaly (Federle et al., 2017.) Hepatomegaly was often noted in the hepatic lymphoma cases. In human, hepatomegaly of lymphoma indicates the degree of invasion of neoplastic lymphocytes (Biemer, 1984). However, hepatomegaly in dogs is detected in several diffuse liver neoplasms including lymphoma, histiocytic sarcoma and mast cell tumour (Cruz-Arambulo et al., 2004; Nyland, 1984; Ramirez et al., 2002; Sato & Solano, 2004). In humans, edge bluntness of the liver is detected in other liver lesions, such as liver fibrosis and inflammation (Afzal et al., 2013). Although not specific for hepatic lymphoma, the finding of both hepatomegaly and edge bluntness may be one of the findings to suspect diffuse liver neoplasms.

The periportal collar sign is caused by dysregulated lymph drainage (Takeda et al., 2015). More than 80% of liver lymph is drained by vessels surrounding the portal veins into the liver hilum (Aspestrand et al., 1991). In dogs with hepatic lymphoma, neoplastic lymphocytes infiltrate surround portal tracts and central veins or wihin sinusoids, depending on form of lymphoma (Cullen, 2017; Keller et al., 2013). The infiltration of neoplastic lymphocytes may cause dysregulated lymph drainage. In this study, periportal collar signs were detected in 60% of dogs with hepatic lymphoma. Although we did not assess the relationship between histopathological findings and periportal collar signs, the periportal collar sign of lymphoma might be influenced by the degree of lymphocyte infiltration. In humans, periportal collar signs are detected in several lesions, including malignant liver tumours, bile duct tumours, hepatic trauma, acute hepatitis, cholangitis, enlarged lymph nodes in the porta hepatis, congestive heart failure and extramedullary hematopoiesis (Takeda et al., 2015). Further studies are needed to determine the relationship between the periportal collar sign and liver lesions.

In humans, solitary or multifocal hepatic lymphoma is usually characterized by lower attenuation than normal liver parenchyma on an unenhanced CT, but diffuse hepatic lymphoma is only characterized by diffused enlargement of the liver (Rajesh et al., 2015; Sanders et al., 1989). In this study, liver lesions with diffuse hepatic lymphoma showed significantly lower attenuation than normal liver. The only report of canine hepatic lymphoma with multiple liver lesions shows low attenuation on CT examination (Chung et al., 2014). In canine hepatic lymphoma, the neoplastic lymphocytes burden large numbers that markedly expanded hepatic sinusoids and compress hepatocytes (Cullen, 2017; Keller et al., 2013; Valli et al., 2017). Low attenuation of lymphoma in pre-contrast phase may be caused by replacement of liver parenchyma by lymphoma and may be influenced by degree of infiltration of lymphoma. On contrast-enhanced CT, nonionic contrast medium exudes to extracellular fluid space of the organs (Bae, 2010). Because lymphomas are high cell density tumours (Colagrande et al., 2018; Haldorsen et al., 2011), lymphoma infiltration may cause the extracellular fluid space to be narrowed. Therefore, canine hepatic lymphoma is indicated by the lower attenuation of liver lesions compared to normal liver on each post-contrast phase. This finding showed the potential to detect liver infiltration of diffuse hepatic lymphoma on CT examination. Further studies are needed in a large population of dogs with hepatic lymphoma and other liver lesions.

CONFLICT OF INTEREST

The authors declare no potential conflicts of interest with respect to the research, authorship or publication of this article.

ACKNOWLEDGEMENT

We thank the staff of the Kinki Animal Medical Training Institute for their help with the manuscript and the care of our patients.

THE ETHICAL STATEMENT

The owners of clinical cases described in this study provided informed consent for the diagnostic procedures, treatment and use of clinical data, such as medical history, imaging studies and histopathological findings for research and publication purposes. Because all diagnostic studies and initiated treatments were part of daily clinical activities, this study could be exempted from submission to the local ethics and welfare committee.

AUTHOR CONTRIBUTIONS

Toshiyuki Tanaka: Conceptualization, data curation, formal analysis, investigation, project administration, validation, visualization and writing-original draft. Hiroki Yamazaki: Data curation, formal analysis, writing-review and editing. Kazuna Ashida: Data curation, writing-review and editing. Yasumasa Iimori: Data curation, writing-review and editing. Keiichiro Mie: Data curation, formal analysis, writing-review and editing. Hidetaka Nishida: Data curation, writing-review and editing. Hideo Akiyoshi: Supervision, writing-review and editing.

DATA AVAILABILITY STATEMENT

The data that support the findings of this study are available from the first author upon reasonable request.

PEER REVIEW

The peer review history for this article is available at https://publons.com/publon/10.1002/vms3.598

ORCID

Toshiyuki Tanaka https://orcid.org/0000-0002-7911-913X
Hiroki Yamazaki https://orcid.org/0000-0002-2613-8169
Hideo Akiyoshi https://orcid.org/0000-0002-5945-0300

REFERENCES

Afzal, S., Masroor, I., & Beg, M. (2013). Evaluation of chronic liver disease: Does ultrasound scoring criteria help? *International Journal of Chronic Diseases*, *2013*, 326231.

Aspestrand, F., Schrumpf, E., Jacobsen, M., Hanssen, L., & Endresen, K. (1991). Increased lymphatic flow from the liver in different intra- and extrahepatic diseases demonstrated by CT. *Journal of Computer Assisted Tomography*, *15*, 550–554.

Bae, K. T. (2010). Intravenous contrast medium administration and scan timing at CT: Considerations and approaches. *Radiology*, *256*(1), 32–61.

Bahr, K. L., Sharkey, L. C., Murakami, T., & Feeney, D. A. (2003). Accuracy of US-guided FNA of focal liver lesions in dogs: 140 cases (2005–2008). *Journal of the American Animal Hospital Association*, *49*(3), 190–196.

Biemer, J. J. (1984). Hepatic manifestations of lymphomas. *Annals of Clinical and Laboratory Science*, *14*(4), 252–260.

Chung, T. - H., Lamm, C., Choi, Y.- C., Lee, J.- W., Yu, D., & Choi, U.- S. (2014). A rare case of hepatic T-cell rich B-cell lymphoma (TCRBCL) in a juvenile dog. *Journal of Veterinary Medical Science*, *76*(10), 1393–1397.

Cohen, J. (1988a). The significance of a product moment r_s. In: J. Cohen (ed.), *Statistical power analysis for the behavioral sciences* (2nd ed., pp. 75–107). Hillsdale: Lawrence Erlbaum Associates.

Cohen, J. (1988b). Chi-square tests for goodness of fit and contingency tables. In: J. J. Cohen (ed.), *Statistical power analysis for the behavioral sciences* (2nd ed., pp. 215–271). Hillsdale: Lawrence Erlbaum Associates.

Colagrande, S., Calistri, L., Grazzini, G., Nardi, C., Busoni, S., Morana, G., & Grazioli, L. (2018). MRI features of primary hepatic lymphoma. *Abdominal Radiology*, *43*(9), 2277–2287.

Cruz-Arambulo, R., Wrigley, R., & Powers, B. (2004). Sonographic features of histiocytic neoplasms in the canine abdomen. *Veterinary Radiology & Ultrasound: The Official Journal of the American College of Veterinary Radiology and the International Veterinary Radiology Association*, *45*(6), 554–558.

Cullen, J. M. (2017). Tumors of the liver and gallbladder. In: J. M. Donald (ed.), *Tumors in domestic animals* (5th ed., pp. 629–631). NJ: John Wiley & Sons, Inc.

Federle, M. P., Tublin, M. E., & Raman, S. P. (2017). Hepatomegaly. In M. P. Federle (ed.), *ExpertDDx: Abdomen and pelvis E-book* (2nd ed., pp. 324–327). US: Elsevier Inc.

Haldorsen, I. S., Espeland, A., & Larsson, E. - M. (2011). Central nervous system lymphoma: Characteristic findings on traditional and advanced imaging. *American Journal of Neuroradiology*, *32*(6), 984–992.

Ippolito, D., Porta, M., Maino, C., Pecorelli, A., Ragusi, M., Giandola, T., Querques, G., Talei Franzesi, C., & Sironi, S. (2020). Diagnostic approach in hepatic lymphoma: Radiological imaging findings and literature review. *Journal of Cancer Research and Clinical Oncology*, *146*(6), 1545–1558.

Keller, S. M., Vernau, W., Hodges, J., Kass, P. H., Vilches-Moure, J. G., Mcelliot, V., & Moore, P. F. (2013). Hepatosplenic and hepatocytotropic T-cell lymphoma: two distinct types of T-cell lymphoma in dogs. *Veterinary Pathology*, *50*(2), 281–290.

Lamb, C. R., Hartzband, L. E., Tidwell, A. S., & Pearson, S. H. (1991). Ultrasongraphic findings in hepatic and splenic lymphosarcoma in dogs and cats. *Veterinary Radiology & Ultrasound: The Official Journal of the American College of Veterinary Radiology and the International Veterinary Radiology Association 32*(3), 117–120.

Lee, S., Yoon, H., & Eom, K. (2019). Retrospective quantitative assessment of liver size by measurement of radiographic liver area in small-breed dogs. *American Journal of Veterinary Research*, *80*(12), 1122–1128.

Maher, M. M., Mcdermott, S. R, Fenlon, H. M., Conroy, D., O'keane, J. C, Carney, D. N., & Stack, J. P. (2001). Imaging of primary non-Hodgkin's lymphoma of the liver. *Clinical Radiology*, *56*(4), 295–301.

Nerschbach, V., Eberle, N., Joetzke, A. E., Hoeinghaus, R., Hungerbuehler, S., Mischke, R., Nolte, I., & Betz, D. (2016). Splenic and hepatic ultrasound and cytology in canine lymphoma: Effects of findings on stagemigration and assessment of prognosis. *Veterinary and Comparative Oncology*, *14*, 82–94.

Nishiura, T., Watanabe, H., Ito, M., Matsuoka, Y., Yano, K., Daikoku, M., Yatsuhashi, H., Dohmen, K., & Ishibashi, H. (2005). Ultrasound evaluation of the fibrosis stage in chronic liver disease by the simultaneous use of low and high frequency probes. *The British Journal of Radiology*, *78*(927), 189–197.

Nyland, T. G. (1984). Ultrasonic patterns of canine hepatic lymphosarcoma. *Veterinary Radiology & Ultrasound: The Official Journal of the American College of Veterinary Radiology and the International Veterinary Radiology Association*, *25*(4), 167–172.

O'brien, R. T. (2007). Improved detection of metastatic hepatic hemangiosarcoma nodules with contrast ultrasound in three dogs. *Veterinary Radiology & Ultrasound: The Official Journal of the American College of Veterinary Radiology and the International Veterinary Radiology Association*, *48*(2), 146–148.

Rajesh, S., Bansal, K., Sureka, B., Patidar, Y., Bihari, C., & Arora, A. (2015). The imaging conundrum of hepatic lymphoma revisited. *Insights Imaging*, *6*(6), 679–692.

Ramirez, S., Douglass, J. P., & Robertson, I. D. (2002). Ultrasonographic features of canine abdominal malignant histiocytosis. *Veterinary Radiology & Ultrasound: The Official Journal of the American College of Veterinary Radiology and the International Veterinary Radiology Association*, *43*(2), 167–170.

Roth, L. (2001). Comparison of liver cytology and biopsy diagnoses in dogs and cats: 56 cases. *Veterinary Clinical Pathology*, *30*(1), 35–38.

Sanders, L., Botet, J., Straus, D., Ryan, J., Filippa, D., & Newhouse, J. (1989). CT of primary lymphoma of the liver. *American Journal of Roentgenology*, *152*(5), 973–976.

Sato, A. F., & Solano, M. (2004). Ultrasonographic findings in abdominal mast cell disease: a retrospective study of 19 patients. *Veterinary Radiology & Ultrasound: The Official Journal of the American College of Veterinary Radiology and the International Veterinary Radiology Association*, *45*(1), 51–57.

Takeda, H., Kamachi, K., Yoshida, T., Miyazono, H., Kuruma, T., & Fujii, S. (2015). Computed tomography findings in acute decompensated heart failure: periportal collar sign and lymphedema in the hepatoduodenal ligament and retroperitoneal space. *Springerplus*, *4*, 286.

Tomasian, A., Sandrasegaran, K., Elsayes, K. M., Shanbhogue, A., Shaaban, A., & Menias, C. O. (2015). Hematologic malignancies of the liver: spectrum of disease. *Radiographics*, *35*(1), 71–86.

Vail, D. M., Pinkerton, M. E., & Young, K. M. (2013). Canine lymphoma and lymphoid leukemias. In: D. Vail (ed.), *Withrow and MacEwen's small animal clinical oncology* (5th ed., pp. 608–638). US: Elsevier Inc.

Valli, V. E., Bienzle, D., & Meuten, D. J. (2017). Tumors of the hemolymphatic system. In: J. M. Donald (ed.), *Tumors in domestic animals* (5th ed., pp. 279–280). NJ: John Wiley & Sons, Inc.

Whiteley, M. B., Feeney, D. A., Whiteley, L. O., & Hardy, R. M. (1989). Ultrasonographic appearance of primary and metastatic canine hepatic tumors. A review of 48 cases. *Journal of Ultrasound in Medicine*, *8*(11), 621–630.

Wrigley, R. H., Konde, L. J., Park, R. D., & Label, J. L. (1988). Ultrasonographic features of splenic lymphosarcoma in dogs: 12 cases (1980-1986). *Journal of the American Veterinary Medical Association*, *193*(12), 1565–1568.

How to cite this article: Tanaka, T., Yamazaki, H., Ashida, K., Iimori, Y., Mie, K., Nishida, H., & Akiyoshi, H. (2021). Computed tomography may detect liver infiltration of canine diffuse hepatic lymphoma. *Veterinary Medicine and Science*, *7*, 2172–2177. https://doi.org/10.1002/vms3.598